Hole Doping of Tin Bromide and Lead Bromide Organic–Inorganic Hybrid Semiconductors

Giancarlo S. Lorena,[1] Hiroyuki Hasegawa,[2,3] Yukihiro Takahashi,[1,2] Jun Harada,[1,2] and Tamotsu Inabe*[,1,2,3]
[1]*Graduate School of Chemical Sciences and Engineering, Hokkaido University, Sapporo 060-0810*
[2]*Department of Chemistry, Faculty of Science, Hokkaido University, Sapporo 060-0810*
[3]*Japan Science and Technology Agency, CREST, Chiyoda-ku, Tokyo 102-0075*

(Received <Month> <Date>, <Year>; CL-<No>; E-mail: inabe@sci.hokudai.ac.jp)

Isomorphous layered A_2MBr_4 perovskites (A = $C_6H_5C_2H_4NH_3^+$ and $C_6H_9C_2H_4NH_3^+$; M = Sn and Pb) semiconductors with energy gaps of 2.5–2.9 eV were prepared. Though the as-grown A_2MBr_4 perovskites displayed lower conductivities than the iodide analogs, they were found to be spontaneously doped. Furthermore, we demonstrated that hole doping is effective to a wide range of A_2MX_4 materials that have sizable valence and conduction bands with tunable band gaps, showing potential as soluble semiconductors.

Solid state electronics are important devices that are encountered in many aspects of our daily life. Subsequent breakthrough in technological innovation is expected to involve the fabrication of more flexible and soluble materials. Metal halide perovskites featuring organic cations are the most promising candidate because the organic part bears solubility and flexibility properties, whereas the inorganic part is expected to possess high charge mobility. An example of a metal halide perovskite is cubic-type $CH_3NH_3PbI_3$, which was recently developed for solar cell applications.[1] To date, the power conversion efficiency achieved by such perovskite-type solar cells exceeds that of dye-sensitized solar cells though the hybrid semiconductor possesses solubility properties. Another example is the tin iodide system that involves layer-type A_2SnI_4 (A = organic ammonium) and cubic-type $CH_3NH_3SnI_3$; both are soluble in organic solvents and feature high electrical conductivity.[2,3] Because their energy gaps are always higher than 1 eV, the high conductivity has been attributed to the onset of spontaneous hole doping in the system.[3] This feature was confirmed by the substantial increase of conductivity observed following artificial doping of Sn^{VI} in the mother crystals. Owing to the high mobility in the tin iodide perovskite framework, as confirmed by the Hall effect measurements,[4] tin iodide perovskites are potential soluble semiconductor candidates. However, their chemical instability limits their practical applications despite their potential in field-effect transistors, as reported.[5]

The relatively high redox activity of iodide is considered to be a factor contributing to the instability of the tin iodide system. Compared with iodide, the redox activity of bromide is lower. However, only the optical properties of A_2SnBr_4 compounds have been reported to date[6] unlike the structural and electrical properties that remain unknown. Therefore, herein, we performed basic structural and electrical characterization of A_2SnBr_4. Additionally, we studied A_2PbBr_4 to compare the effect of the redox activity of the metal. The findings showed that both as-prepared organic–inorganic hybrids are doped semiconductors, and that the artificial doping enhanced their conductivity. This study provides important insights into controlling the electronic properties of this class of material that has great potential in low-cost devices prepared via simple fabrication strategies.

To prepare the layered A_2MBr_4 perovskites (M = Sn and Pb), two organic cations were selected: $C_6H_5C_2H_4NH_3^+$ (phenylethylammonium; PEA) and $C_6H_9C_2H_4NH_3^+$ (2-(1-cyclohexenyl)ethylammonium; CEA). Yellow platelet crystals of A_2SnBr_4 were obtained by slow cooling of the ethanol-based solution. Colorless platelet crystals of A_2PbBr_4 were obtained from the dimethylformamide/$CHCl_3$ solution. Details of the experiments including other measurements can be obtained from the Supporting Information.[7]

All crystals obtained i.e., $(PEA)_2SnBr_4$, $(CEA)_2SnBr_4$, $(PEA)_2PbBr_4$,[8] and $(CEA)_2PbBr_4$ are isomorphous.[7] As a representative, the structure of $(PEA)_2SnBr_4$ is shown in Figure 1.

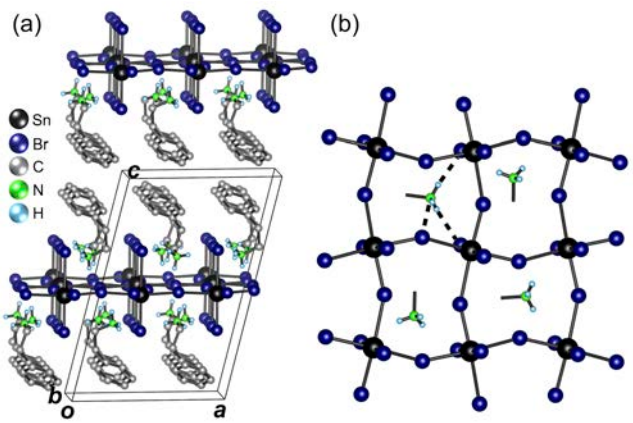

Figure 1. (a) Perspective view of the unit cell and (b) organic–inorganic interface of $(PEA)_2SnBr_4$ viewed along the *c*-axis showing H-bonding between NH_3 and $SnBr_6$ octahedra. Crystal data are as follows: triclinic *P*1-; a = 11.526(1), b = 11.634(1), c = 17.510(1) Å; α = 80.449(2), β = 74.634(2), γ = 89.953(2)°; V = 2230.5(3) Å^3; and Z = 4.

A typical monolayer structure of the metal halide perovskite in which extended two-dimensional corner-shared MBr_6 octahedra were alternated by a bi-layer of organic cations of PEA or CEA was observed. In the inorganic layer, these octahedra are connected distortedly in in-plane directions, leading to the zigzag arrangement of the metal–halogen–metal linkage (Figure 1b). $(PEA)_2SnBr_4$ and $(CEA)_2SnBr_4$ displayed similar Sn–Br bond lengths and Sn–Br–Sn bond angles. The lead bromide-based compounds also

displayed similar Pb–Br bond lengths and Pb–Br–Pb bond angles. The comparable bond lengths and angles[7] have important implications in the band structure of these compounds. The ammonium heads of the organic layers formed hydrogen bonds with the bridging and terminal halogens of the metal bromide octahedra.

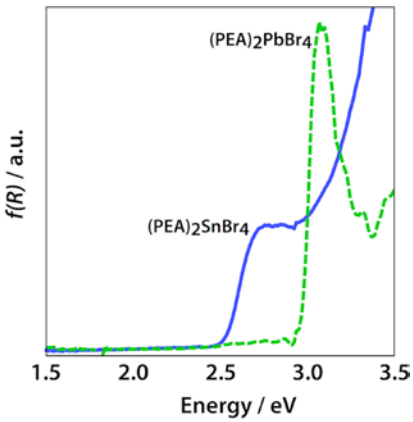

Figure 2. Diffuse reflectance spectra of $(PEA)_2SnBr_4$ and $(PEA)_2PbBr_4$. The reflectivity was converted to the Kubelka-Munk function, $f(R)$, corresponding to the absorption.

Figure 2 shows the diffuse reflectance spectra of $(PEA)_2SnBr_4$ and $(PEA)_2PbBr_4$. The optical band gap (E_G) of $(PEA)_2SnBr_4$ is 2.5 eV and that of $(PEA)_2PbBr_4$ is 2.9 eV. Similar E_G values were obtained for $(CEA)_2SnBr_4$ and $(CEA)_2PbBr_4$.[7]

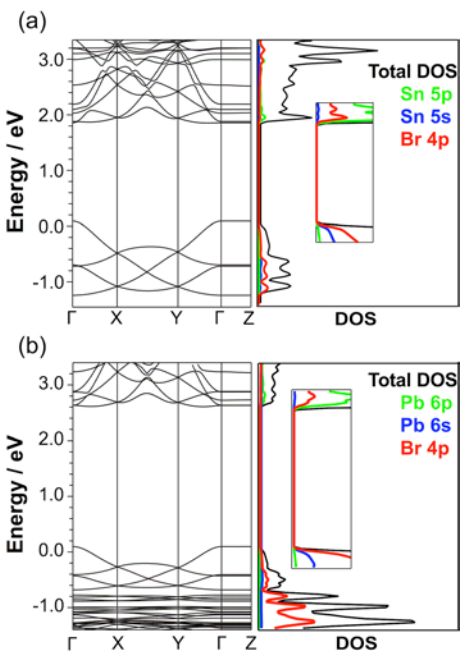

Figure 3. Calculated band dispersion (left) and density of states, (DOS, right) (inset shows magnification of the valence band and conduction band edge) of (a) $(PEA)_2SnBr_4$ and (b) $(PEA)_2PbBr_4$.

Figure 3 shows the theoretically calculated electronic band structures of these compounds.[7,10] The calculated band gaps of $(PEA)_2SnBr_4$ and $(PEA)_2PbBr_4$ were ~2.0 and 2.5 eV, respectively. It should be noted that calculated E_G values, using the first principle GGA (generalized gradient approximation) calculation, are usually underestimated.[3b,9] Therefore, despite the small discrepancies between the optical gaps and calculated gaps, qualitative evaluation of the nature of the electronic systems in these compounds can be performed. In a given metal halide system, the calculated band gaps and valence band widths appear to be very similar.[7] In A_2SnBr_4 and A_2PbBr_4, the metal p orbitals contribute to the bottom of the conduction band. Upon replacement of the tin atom with lead, the energy level of the bottom of the conduction band increased owing to the higher energy level of the Pb 6p orbital. However, the top of the valence band remained relatively the same because of the large contribution from the Br 4p orbital in the metal bromide system. Thus, the band gap values of the tin bromide-based perovskites are narrower than those of the lead bromide-based perovskites.

The differences in the band gaps of A_2MBr_4 compounds are roughly correlated with the resistivity of the compounds at room temperature. The resistivity values of the wide-gap lead bromides are ~10^{11} Ω cm, whereas those of the tin bromides with narrower gaps are ~10^9 Ω cm, as shown in Table 1.

Table 1. Room temperature resistivity (Ω cm) of the as-grown and doped crystals

	$(PEA)_2SnBr_4$	$(CEA)_2SnBr_4$	$(PEA)_2PbBr_4$	$(CEA)_2PbBr_4$
As-grown	7.1×10^8	4.9×10^9	1.4×10^{11}	6.8×10^{11}
Doped	8.1×10^6	5.9×10^7	2.2×10^9	9.3×10^9

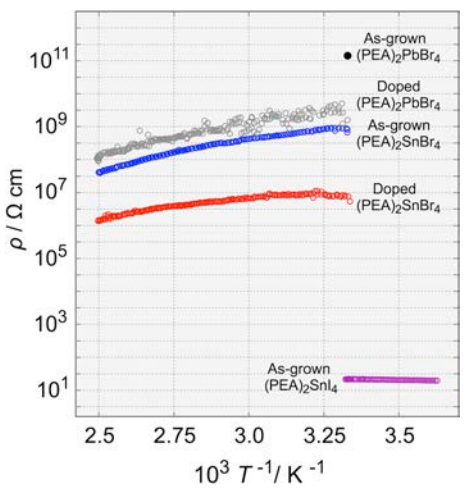

Figure 4. Temperature dependence of resistivity of the as-grown and doped $(PEA)_2SnBr_4$ and $(PEA)_2PbBr_4$ crystals. For comparison, the reported data[3a] of the as-grown $(PEA)_2SnI_4$ crystals are also shown.

To examine the effect of artificial doping on these materials, we synthesized doped perovskite crystals using $Sn^{IV}Br_4$ for the tin-based systems and $Pb^{IV}(OCOCH_3)_4$ for the lead-based materials.[7] The resistivity values of the doped crystals[7] are shown in Table 1. Figure 4 shows the temperature dependence of resistivity of the as-grown and doped $(PEA)_2SnBr_4$ and $(PEA)_2PbBr_4$ crystals, along with that of the close analog of $(PEA)_2SnI_4$, which is highly conducting due to spontaneous hole doping.[3a] The temperature-dependent resistivity profiles of $(PEA)_2SnBr_4$ and $(PEA)_2PbBr_4$ crystals suggest a thermally activated

behavior. The activation energy (E_A) values of the conduction of the as-grown and doped $(PEA)_2SnBr_4$ crystals are 0.32 and 0.21 eV, respectively. Similarly, for the doped $(PEA)_2PbBr_4$, an activation energy of 0.32 eV was obtained.[11]

Considering the E_G values of $(PEA)_2SnBr_4$ (2.5 eV) and $(PEA)_2PbBr_4$ (2.9 eV), it is reasonable to assume that conductivity in these crystals is extrinsic. Because the valence band is occupied by the Sn 5s or Pb 6s and Br 4p orbitals, the vacant acceptor levels may form upon oxidation of the MBr_4^{2-} units. An enhanced conductivity owing to artificial doping with M^{IV} was thus observed, suggesting that the carriers in these systems are holes.

This characteristic was also observed for the tin iodide-based perovskites.[3] However, comparison of the above results with the transport properties of the as-grown $(PEA)_2SnI_4$ crystals in Figure 4 revealed a significant difference; its room temperature resistivity is only 40 Ω cm and the temperature dependence is not thermally-activated behavior.[3a] Compared with $(PEA)_2SnBr_4$, aside from the contribution of the Sn 5s orbital to the top of the valence band, $(PEA)_2SnI_4$ will have a higher energy level at the top of the valence band because the energy level of the I 5p orbital is higher than that of the Br 4p orbital (Figure 5).

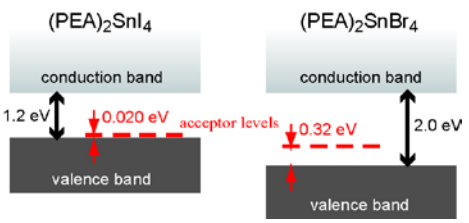

Figure 5. Schematic representation of the calculated band structures of $(PEA)_2SnI_4$ and $(PEA)_2SnBr_4$ and acceptor levels formed in the band gap..

However, this difference in the band gap values cannot explain the difference in the conductivity observed between these systems because tin iodide is six orders of magnitude more conductive than tin bromide. The conductivity of semiconductors can be determined according to the general equation: $\sigma = qn\mu$, where n is the number of current-carrying species, μ is the mobility of these carriers, and q is the charge of the carriers. Band calculation shows the comparable valence band widths of $(PEA)_2SnBr_4$ and $(PEA)_2SnI_4$, suggesting that the carrier mobility is comparable as well. If we assume the charge of the carriers to be the same, we can conclude that the difference in conductivity between tin iodide and tin bromide perovskites is due to the difference in the number of carriers, n. It should be noted that E_A of the as-grown $(PEA)_2SnI_4$ crystals is considerably smaller (0.020 eV)[3a] when compared with that of the as-grown $(PEA)_2SnBr_4$ crystals (0.32 eV). If the number of acceptor sites, n_A, is comparable, n at 300 K is estimated to be five orders of magnitude higher in $(PEA)_2SnI_4$ than in $(PEA)_2SnBr_4$, assuming $n = n_A\exp(-E_A/kT)$. Because the ratio of n is mostly identical to the conductivity ratio, the spontaneous generation of comparable amounts of acceptor sites is expected in the as-grown $(PEA)_2SnBr_4$. The artificial doping reduces the resistivity by two orders of magnitude and the E_A to 2/3. As assumed for A_2SnI_4, μ is considered to be in the range of 1–10 $cm^2\ V^{-1}\ s^{-1}$. Therefore, we can conclude that the dopant concentration in the doped $(PEA)_2SnBr_4$ is comparable to that in the doped $(PEA)_2SnI_4$; the doping level must be lower than 1%, and can not be controlled by the initial dopant concentration in the solution for the artificial doping.[7]

The higher resistivity of both the as-grown and doped $(PEA)_2PbBr_4$ can also be explained as discussed above. Therefore, the vacant Pb 6s orbital of the dopant is considered to contribute to the formation of acceptor levels. The doping level may also be comparable to the tin bromide system.

In conclusion, though the bromide analog of $(PEA)_2SnI_4$ i.e., $(PEA)_2SnBr_4$ showed significantly lower conductivity in the as-grown state, both the iodide- and bromide-based perovskites were found to be spontaneously doped to a small extent. The exceptionally high conductivity of A_2SnI_4 was attributed to the extremely small energy difference between the top of the valence band and acceptor levels. This study demonstrates that hole doping is effective for a wide range of A_2MX_4 materials with M = Sn and Pb and X = I and Br. Because the bromides are relatively more stable than the iodides and have sizable valence and conduction bands with tunable band gaps, they show promise as soluble semiconductors.

This work was supported in part by a Grant-in-Aid for Scientific Research from the Ministry of Education, Culture, Sports, Science and Technology, Japan. We are grateful to Prof. M. Wakeshima for his assistance in the band structure calculations.

References and Notes

1 A. Kojima, K. Teshima, Y. Shirai, T. Miyasaka, *J. Am. Chem. Soc.* **2009**, *131*, 6050; M. M. Lee, J. Teusher, T. Miyasaka, T. Murakami, H. Snaith, *Science* **2012**, *338*, 643; M. Liu, M. Johnston, H. Snaith, *Nature* **2013**, *501*, 395; D. Liu, T. L. Kelly, *Nature Photon.* **2014**, *8*, 133.

2 D. B. Mitzi, C. A. Feild, W. T. A. Harrison, A. M. Guloy, *Nature* **1994**, *369*, 467; D. B. Mitzi, *Progress Inorg. Chem.* **1999**, *48*, 76. D. B. Mitzi, C. A. Feild, Z. Schlesinger, R. B. Laibowitz, *J. Solid State Chem.* **1995**, *114*, 159.

3 a) Y. Takahashi, R. Obara, K. Nakagawa, M. Nakano, J. Tokita, T. Inabe, *Chem. Mater.* **2007**, *19*, 6312; b) Y. Takahashi, R. Obara, Z. Lin, Y. Takahashi, T. Naito, T. Inabe, S. Ishibashi, K. Terakura, *Dalton Trans.* **2011**, *40*, 5563.

4 Y. Takahashi, H. Hasegawa, Y. Takahashi, T. Inabe, *J. Solid State Chem.* **2013**, *205*, 39.

5 C.R. Kagan, D.B. Mitzi, C.D. Dimitrakopoulos, *Science* **1999**, *286*, 945; D. B. Mitzi, C. D. Dimitrakopoulos, L. S. Kosbar, *Chem. Mater.* **2001**, *13*, 3728.

6 G. C. Papavassiliou, J. B. Koutselas, D. J. Lagouvardos, Z. Naturforsch. **1993**, *48b*, 1013; G. C. Papavassiliou, J. B. Koutselas, *Synth. Met.* **1995**, *71*, 1713.

7 Supporting Information is available electronically on the CSJ-Journal Web site, http://www.csj.jp/journals/chem-lett/index.html.

8 The structure was found to be the same with that reported; K. Shibuya, M. Koshimizu, F. Nshikido, H. Saito, S. Kishimoto, *Acta Crystallogr. Sect. E* **2009**, *65*, m1323.

9 Y. Chang, C. Park, *J. Korean Phys. Soc.* **2004**, *44*, 889; Y. Li, C. Lin, G. Zheng, Z. Cheng, H. You, W. Wang, J. Lin, *Chem. Mater.* **2006**, *18*, 3463; S. Sourisseau, N. Louvain, W. Bi, N. Mercier, D. Rondeau, F. Boucher, J.-Y. Buzare, C. Legein, *Chem. Mater.* **2007**, *19*, 600.

10 P. Blaha, K. Schwarz, G.K.H. Madsen, D. Kvasnicka, and J. Luitz, Wien2k, *An Augmented Plane Wave + Local Orbital Program for Calculating Crystal properties*, Technische Universität Wien, Austria, 2001. ISBN 3-9501031-1-2

11 The reliable temperature dependence of the resistivity for the as-grown $(PEA)_2PbBr_4$ crystal could not be obtained due to large signal-to-noise ratios in the current-voltage plots.